Perspectives for the AMBER Beam Combiner

Antoine Mérand[a], Stan Stefl[a], Pierre Bourget[a], Andres Ramirez[a], Fabien Patru[a], Pierre Haguenauer[a], Stéphane Brillant[a] and the AMBER Instrument Operation Team[a,b] (IOT)

[a] ESO Chile; Cerro Paranal Observatory, Antofagasta Region, Chile
[b] ESO Headquarters; Garching, Germany

ABSTRACT

The Astronomical Multi-BEam Recombiner (AMBER), has been operational at the Very Large Telescope Interferometer (VLTI) for many years. We present here some of the constant improvements we have been providing while still operating the instrument, with a heavy load of visitor and service observing programs, most of the nights of the year. In particular, we present here improvements regarding the spectral calibration and correction of the atmospheric loss in squared visibility due to path difference jitter, allowing the instrument to achieve greater precision.

Keywords: technique: interferometry; technique: spectroscopy; near-infrared;

1. INTRODUCTION

AMBER, the astronomical Multi-BEam Recombiner,[1] is the one of the two beam combiners currently operational at the European Southern Observatory's VLTI. It operates in the near-infrared, (J, H and K bands), combines 3 telescopes simultaneously and offers spectral dispersion of approximately 35, 1500 or 15000. AMBER is used with various configurations: it can recombine 3 Unit Telescopes (8.2m in diameter) or 3 Auxiliary telescopes (1.8m in diameter), with or without active fringe tracking (using the current VLTI 3 telescopes fringe tracker, FINITO[2]). AMBER has been offered to the community in 2005 We present here two works in progress: 1) the spectral calibration and spectrum extraction and 2) the debiasing of the atmospheric optical path difference jitter using FINITO real-time recording.

2. SPECTRAL CALIBRATION

In spectro-interferometry, the wavelength has two different roles. First of all, the wavelength λ defines, with the projected baseline B, the spatial frequency B/λ. The accuracy of the spatial frequency can be a limitation for accurate measurements. Secondly, the spectral dispersion is also involved as in a classical spectrograph, to resolve absorption and/or emission lines. Accurate spectral calibration is required in some cases, for instance when a spectral line is highly resolved and distorted by a radial velocity field: an accurate spectral calibration is required to study this velocity field. This is the case for AMBER, particularly in medium and high resolution modes.

For AMBER, the case of Low resolution (LR) and the higher resolutions (know as Medium and High resolution, MR and HR) is different regarding the spectral calibration. We will first address the Low resolution.

Further author information: (Send correspondence to A. Mérand)
A. Mérand: E-mail: amerand@eso.org

2.1 Low resolution spectral calibration

Low Resolution (LR) mode disperses simultaneously the near infrared J, H and K bands, with a dozen or so pixels per band. The dispersion is too low to distinguish telluric lines from the Earth atmosphere. This is the case for MR (medium resolution) and HR (high resolution), which we will investigate in the next section. Currently, the wavelength calibration is based on the localization of the boundaries of the H band in the spectrum and the known spectral dispersion of the prism used in LR. In AMBER, each band (J, H and K) is separated at the entrance of the instrument, injected in modal filters (single mode fibers) and recombined/superimposed later on the entrance slit of the spectrograph, with an overlap corresponding to less than half a pixel of the detector. This later tolerances in assured by a coalignment done every day using the 0-order of the medium resolution grism. It means that once the H band is localized, one expects an offset less than 0.5 pixel between H and K, due to not-superimposed beams (HK co-alignment).

In practice, it has been suspected that the LR-K band is not accurate. For example, Wittkowski et al. (2008)[3] noticed a $0.1\mu m$ offset between the measured spectrum in LR-K of 4 stars and synthetic spectra taking into account the K band filter and the atmospheric transmission. This corresponds to approximately to 3 pixels offset. Using the measured transmission of the different dichroics and the single mode fibers, one can try to model the spectrum observed by AMBER. This modeling should take into account the transmission of the Earth's atmosphere and the spectrum of the star (in LR, a simple black body is enough). Because we want to get the dispersion law, such model should introduce a correction to the spectral dispersion given by the observation software. Finally, we allow for an unknown chromatic dispersion, modeled using a polynomial function of the wavelength.

By doing so, we find no departure of the dispersion law in H band (see Figure 1, left). Namely, we find:

$$\lambda_c = 1.65 + [0.003 \pm 0.002] + (\lambda - 1.65) \times [0.98 \pm 0.02] \text{ [for LR} - \text{H]}$$

where λ_c is the corrected wavelength (in microns), and λ is the wavelength given in the AMBER FITS file's header, estimated by the control software. This is not a surprise, since this is how the spectral calibration is currently done. We tried to fit also a curvature to wavelength correction, but it is not significant: the correction in term of $(\lambda - 1.65)^2$ is 0.3 ± 0.4.

It is to be noticed that in these kind of fit, there is usually a a strong coupling between the transmission shape and the dispersion law. In the case of the H band alone, the fit is efficient because the dispersion law is in practice constrained by the limits of the H band filter. For the K band, as the end of the K band is not recorded, leading to an uncertainty in the K band dispersion law. However, a careful modeling of the K band transmission reveals that the 0.1 micron offset described by some authors might not be real. Indeed, these authors did not take into account the spectral transmission of the K band single mode fibers in silicate glass, which have a strong reduction of the transmission above 2.2 microns. A full fit in the J, H and K band leads, once again, to a negligible dispersion correction (Figure 1, right):

$$\lambda_c = 1.65 + [-0.017 \pm 0.006] + (\lambda - 1.65) \times [1.02 \pm 0.03] \text{ [for LR} - \text{JHK]}$$

As a conclusion, we can say that the current spectral calibration delivered by AMBER in LR mode is probably accurate at the 1 or 2% level, assuming that the borders of the H Band's filter are accurate, as described in the technical dumentation accompanying AMBER (ESO internal document).

A definitive answer will be brought when our efforts to redesign the calibration source will lead to the inclusion of a spectral lamp (Th-Ar or Ne) which, according to preliminary tests, allows an accurate spectral calibration, independent from modeling and fitting the spectral transmission of the instrument.

2.2 Medium and high resolution spectral calibration

In medium (R$\approx$ 1500) and high (R$\approx$ 15000) spectral resolutions, the situation is easier since telluric lines are visible in the spectrum. Using the same approach developed for traditional spectroscopy, one can use synthetic telluric spectra. Using a library of synthetic spectra created at high resolution (R$\approx$ 100000, for the infrared

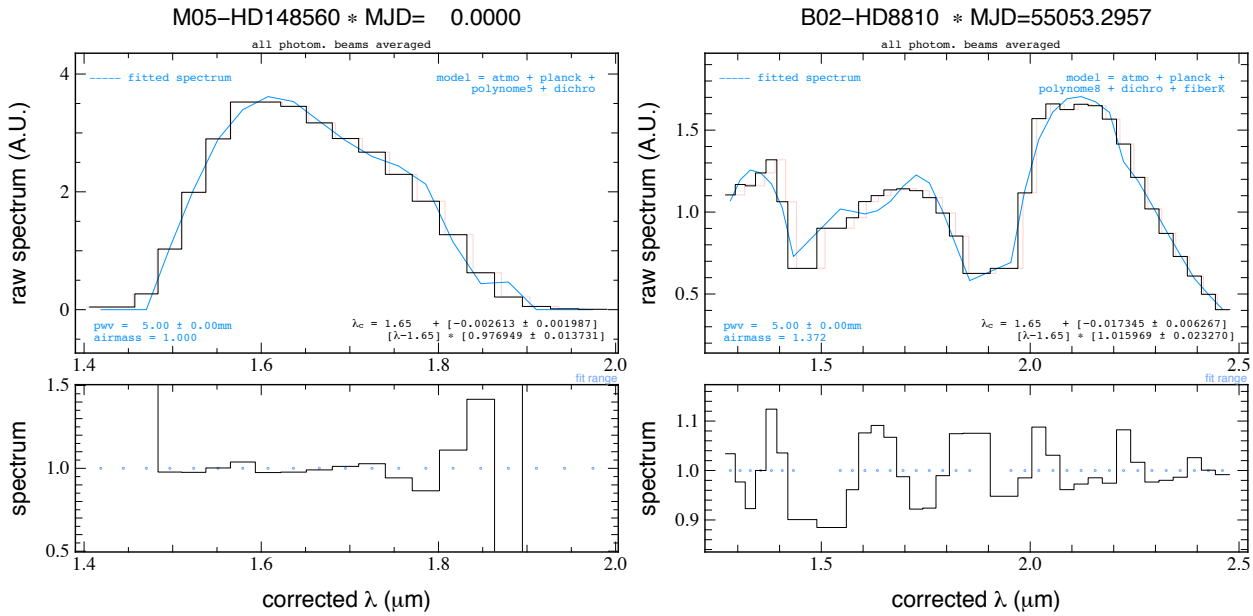

Figure 1. Transmission and dispersion law fit in LR-H mode (left) and LR-JHK (right). The continuous line is the model transmission; the step-line if the AMBER spectrum with corrected dispersion law; the light step-line is the spectrum before the dispersion correction. In both cases, the correction in spectral dispersion is negligible.

spectrograph CRIRES, Smette & Sana, 2010, *in preparation*) for different amounts of precipitable water vapor (PWV), we can model the transmission, calibrate the spectral dispersion and, as a by-product, extract the spectrum from the AMBER photometric data.

The dispersion calibration is very accurate using this technique, due to the large number of telluric lines (Figure 2). In high resolution, the precision of the spectral calibration is of the order of 0.000022 microns for the setup surrounding the Bracket gamma line (*lambda* ≈ 2.17 μm, which corresponds to 0.2 pixel, or 3km/s. In medium resolution, the precision is 0.8 pixel, or 80km/s. It is proportionally worst, since the telluric lines are marginally resolved, whereas they are nicely resolved in HR. Again, like in LR mode, the spectral dispersion provided by the AMBER observing software is quite accurate. The main difference is the presence of an offset of many pixels, otherwise the dispersion law is correct at a few percent level. It is to be noted that currently, AMBER zero point of the MR and HR spectral calibration is based on the position of the stepper motor that drives the grisms' wheel, which explains the presence of the offset.

It is not clear how stable the spectral calibration is, in particular how reliable is the central wavelength correction in MR and HR modes. In order to obtain even more accurate spectral calibration, the use of the already mentioned spectral lamp is under investigation, in order to directly calibrate the wavelength table. The first results look promising.

2.3 Simple example of spectro-interferometry

An obvious by-product of the spectral calibration using a fit of the telluric lines outside the photospheric lines is an extracted normalized spectrum of the object. In the next section we present a new application combining both the extracted normalized spectrum and the visibility spectrum.

Apart from the obvious case of studying the dynamic of a feature resolved by spectro-interferometry, we propose here a simple, yet novel, application of spectro-interferometry. The idea of this approach is to address the detection of resolved circumstellar envelops (CSE). We will use three specific features, which represent the main hypothesis under which the following method works:

- at the observed baseline, the CSE is fully resolved.

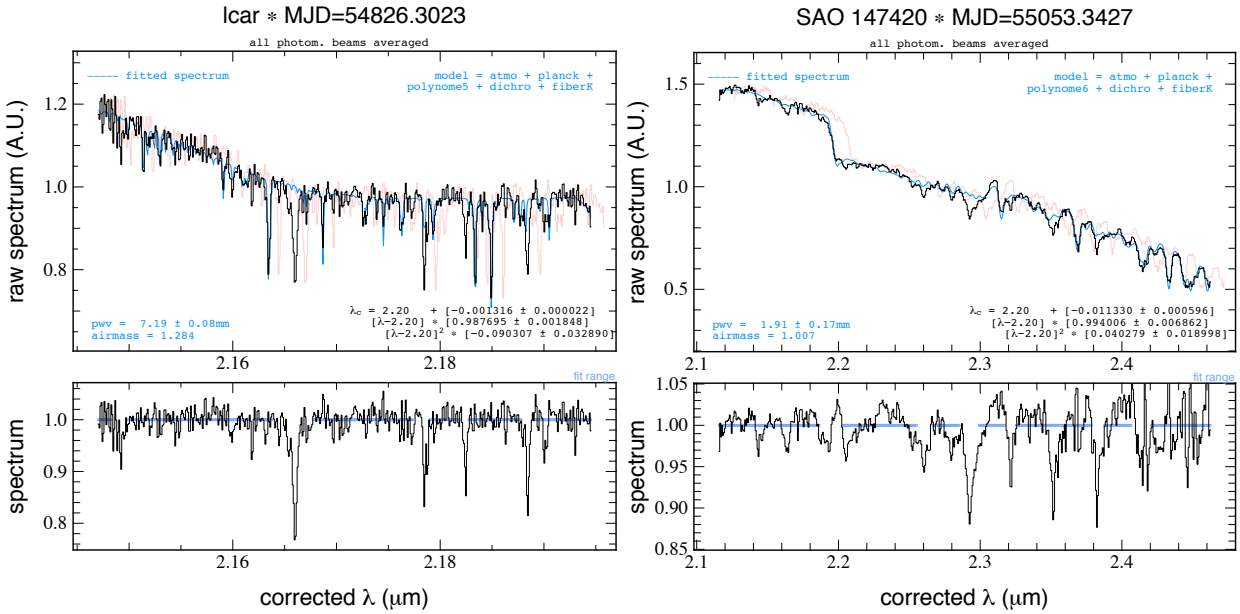

Figure 2. Same as figure 1, in high resolution 2.170 μm (left) and in medium resolution 2.3μm (right). The lower panels show the spectra normalized to the continuum, with corrected spectral dispersion. On the left, one can see that the continuum fitting is perturbed by the CO lines (2.3 microns and above).

- the star is barely resolved, which means that the visibility does not have stellar features in the lines.
- the spectrum of the CSE does not contain spectral lines.

In the following, we will denote F for fluxes and V for interferometric visibilities; $F_\star$ refers to the star component and $F_{\rm CSE}$ to the envelop; $V^c_\star$ denoted the continuum value, i.e. outside the photospheric lines.

Absil et al. (2006)[4] pioneered the approach of measuring the photometric excess of completely resolved CSE (debris disks in this case) by comparing the accurately measured visibility of a star to the expected one. The deficit is interpreted as a bias due to the photometric excess $F_{\rm CSE}/(F_{\rm CSE}+F_\star)$. In the case we are going to present, we lack the accurate knowledge of the expected visibility, hence we cannot measure the deficit. However, because the star has absorption lines, its flux ratio with the CSE varies between the lines and the continuum. We make use of this effect to extract a photometric measurement. Using our symbol convention, we can write the normalized spectrum S, as well as the normalized visibility S_V (normalized to the visibility outside the spectral photospheric lines):

$$S = \frac{F_\star + F_{\rm CSE}}{F^c_\star + F^c_{\rm CSE}} \tag{1}$$

Owing to the linearity of the visibility, we can express the visibility of the star surrounded by the CSE as:

$$V = \frac{V_\star F_\star + V_{\rm CSE} F_{\rm CSE}}{F_\star + F_{\rm CSE}} \tag{2}$$

Assuming the visibility of CSE is negligible, the continuum-normalized visibility is then:

$$S_V = V/V^c = \frac{V_\star F_\star}{V^c_\star F^c_\star} \times \frac{F^c_\star + F^c_{\rm CSE}}{F_\star + F_{\rm CSE}} \tag{3}$$

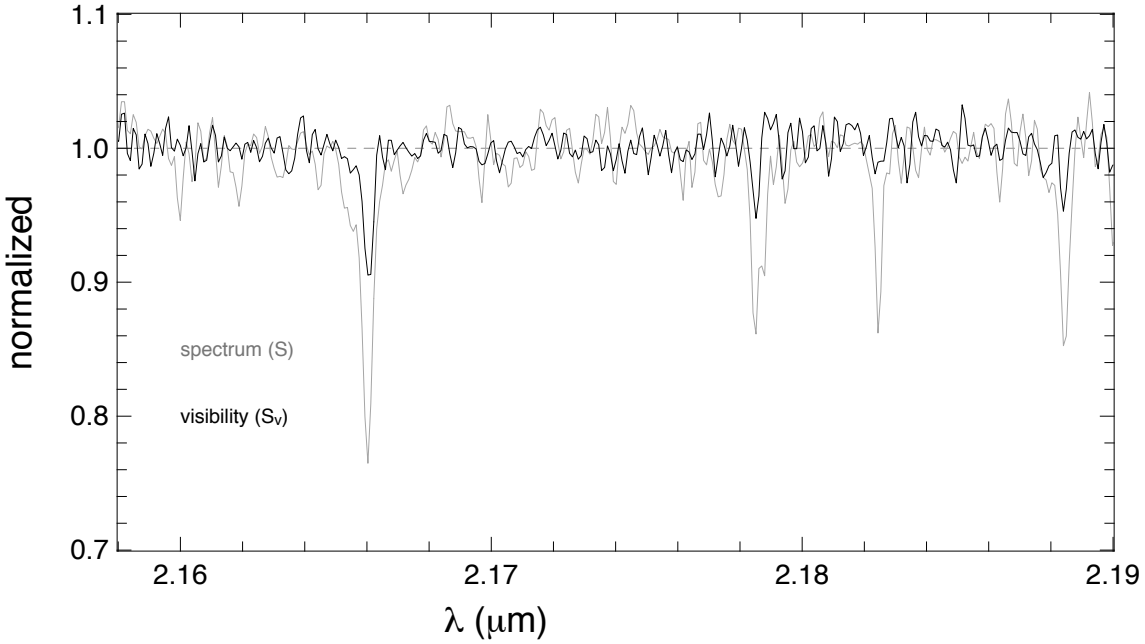

Figure 3. Attempt to detect the CSE around the Cepheid ℓ Car using spectro-interferometry (article in preparation). Normalized spectrum (gray) and normalized visibilities (black) as a function of wavelength. The most preeminent line is Brackett-γ (2.166 microns) which might have a signal in visibilities because its features in CSE. Our interest is here on the three other photospheric lines (2.178, 2.182, 2.188 microns in particular). At the level of precision of these data, the known CSE at about 4% in relative flux,[5] seems out of reach.

We can remove the contribution of CSE by multiplying it by the normalized spectrum S:

$$S \times S_V = \frac{V_\star F_\star}{V_\star^c F_\star^c} \tag{4}$$

Now, if we assume that the $V_\star = V_\star^c$, which means that in the photospheric lines the star as the same morphology as in the continuum, and that the visibility of the continuum is negligible, we can obtain, by combining the spectrum and the visibility spectrum, the true normalized spectrum of the star:

$$S \times S_V = \frac{F_\star}{F_\star^c} \tag{5}$$

Using a little more algebra, we can actually also extract the flux ratio between the star and it CSE, which is a very important observable. Indeed, we can derive:

$$S \times \frac{Sv - 1}{S - 1} = \frac{F_{\rm CSE}^c}{F_\star^c + F_{\rm CSE}^c} \tag{6}$$

Of course, the use of the later expression is limited to the region on the spectra where photospheric lines are present: the quantity $S - 1$ is equal to zero outside photospheric line, so the above quantity diverges in in the continuum.

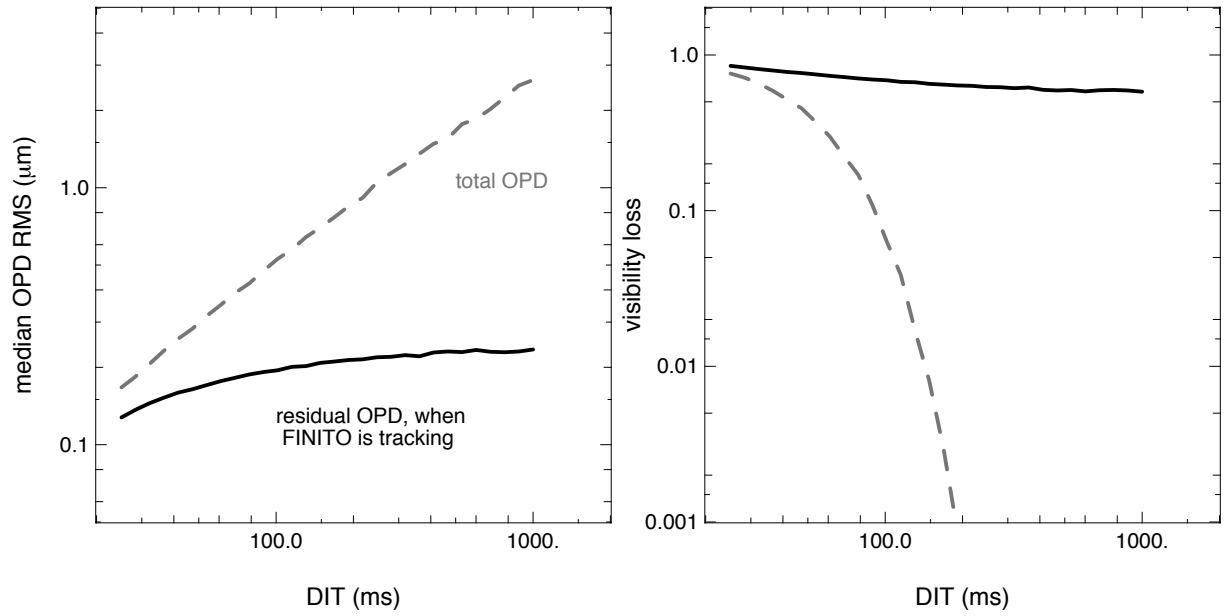

Figure 4. **Left:** OPD RMS extracted by averaging the FINITO recordings for different time spans, corresponding to the integration of the interferograms. The dash line is the atmospheric jitter and the continuous line is the residual jitter after correction. **Right:** the corresponding expected V^2 loss $e^{-(2\pi\sigma_{\rm OPD}/\lambda)^2}$ in K Band for the natural and residual RMS ($\lambda = 2.0$ μm. The usefulness of fringe tracking is obvious in this case, as it allows long exposures (several seconds).

3. ATMOSPHERIC VISIBILITY BIAS CORRECTION USING REAL TIME FRINGE TRACKER RECORDS

3.1 Context

It is well known that atmospheric optical path difference (OPD) jitter leads to a reduction of the interferometric squared visibility. If $\sigma_\phi = 2\pi\sigma_{\rm OPD}/\lambda$ is the phase jitter, the attenuation in squared visibility is (Colavita 1999[6]):

$$\Gamma = e^{-\sigma_\phi^2} \tag{7}$$

σ_ϕ depends on the characteristics of the atmospheric turbulence and should be computed over the integration time considered (the integration time of the interferogram), as can be seen on Fig. 4. This effect restricts the uses of optical interferometry to short exposures (typically of the order of ten millisecond in the optical regime) because for long exposure times —DIT, for detector integration time— the visibility is too low. Apart from the correction for the instrumental visibility loss, this varying loss (because the turbulence characteristics, especially the coherence time in this case, vary in time) is the main reason why interferometric observations require use of stellar calibrators, with predictable visibility, in order to calibrate the average loss assuming this loss is stable enough.

If one needs longer exposures, which is the case for high spectroscopic resolution, the solution is to use a fringe tracker which measures and corrects the OPD jitter in order to drastically reduce σ_ϕ on large time scale, typically a few seconds (see Fig. 4). Another problem is that the jitter can vary a lot from an interferogram to another: this can add a very large scatter which is dreadful to estimate a precise visibility. This is the case for AMBER, which integrates fringes during at least 25ms (minimum DIT in low resolution mode, corresponding to the physical time it takes to read the detector twice for a correlated measurement).

3.2 Frame to frame correction of the visibility bias

A new feature at VLTI, called RMN recorder (Ring Memory Network recorder, Abuter et al., this proceedings), allows to record the parameters measured by FINITO every millisecond while we observe with the AMBER

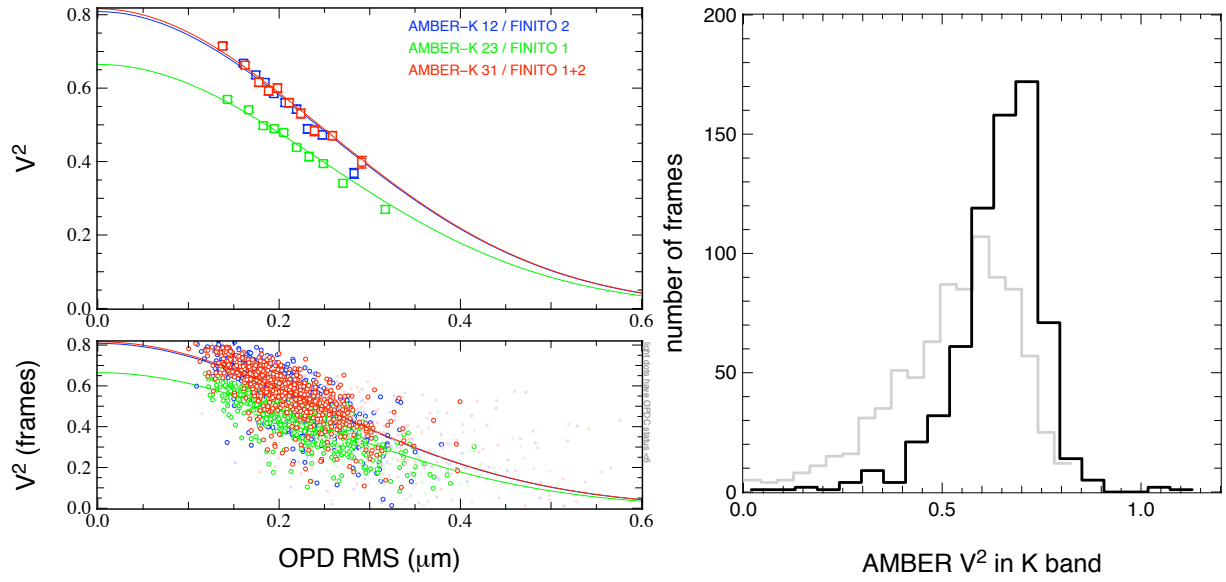

Figure 5. **Right**, bottom panel: squared visibilities of AMBER frames in K band with DIT=200ms over minutes, as a function of the computed jitter from FINITO data the light dots corresponds to frames for which the fringe tracking loop was open. The top panel shows the averages over bins of OPD RMS. The three colors are for the 3 baselines. The line is the expected loss ($\sigma_\phi = 2\pi\sigma_{\rm OPD}/\lambda$), with the 0-RMS point adjusted. **Left**: histograms of squared visibilities for one baseline. Gray is is straight out of the data reduction software, the dark line if for visibilities corrected from the expected bias, based on the OPD RMS.

beam combiner. Using this precious recordings, we can compute several things for each AMBER frame, which uses an integration over DIT=25ms to DIT=10s typically:

- whether or not the active fringe tracking loop was closed or not;
- compute the residual jitter RMS as seen by AMBER.

This allows to select frames for which the fringe tracking loop was closed and correct each frame of the visibility bias. On Fig. 5, one can see a direct application of the frame-to-frame correction. By selecting frames for which the loop was closed and computing for each frame the visibility bias, we can fit the measured visibilities as a function of the jitter.

This approach has two advantages:

- it increases the **precision** by reducing the scatter of the data points;
- it increases the **accuracy** because by extrapolating the visibility to 0-jitter, one extracts a visibility largely independent from the OPD jitter.

We have not yet verified this in an sufficiently extended way to be able to provide quantitative estimations of the accuracy. However, we can report that visibilities recorded for various DITs show encouraging level of precision (small formal error bars) and accuracy (consistency). By defining the visibility as the 0-jitter fitted to the data "V^2 as a function of measured OPD jitter", we potentially remove any influence of the OPD jitter, assuming this later is perfectly measured by the fringe tracker. 0-jitter Visibilities estimated at different DITs (Tab. 1) still show a decrease as the DIT increase, but in proportion much smaller than without fringe tracker or by simple averaging. This can be explained as follow: if FINITO under estimate the OPD jitter, which it will do in case of fringe's jump, one will have artificially low measured visibility for an apparently low jitter, driving the 0-jitter fit to lower values. This means that, for future applications, one should probably keep observing stellar calibrators and keep the same DIT for the calibrators and the unknown targets.

Table 1. table Visibility measured and debiased using FINITO records. The visibility shown here is the 0-jitter fitted to the data "V^2 as a function of measured OPD jitter".

DIT (ms)	V^2_{12}	V^2_{23}	V^2_{31}
25	0.895 ± 0.003	0.708 ± 0.004	0.876 ± 0.004
50	0.867 ± 0.006	0.685 ± 0.002	0.883 ± 0.002
200	0.813 ± 0.009	0.673 ± 0.005	0.833 ± 0.005
400	0.825 ± 0.008	0.626 ± 0.003	0.830 ± 0.009
800	0.820 ± 0.010	0.669 ± 0.005	0.817 ± 0.007

4. CONCLUSIONS AND PERSPECTIVES

We have presented two new developments concerning the AMBER instrument: improvements of the spectral calibration and improvement of the precision and accuracy of the visibilities' measurements. The first improvements provide an absolute spectral calibration at the 3km/s and 80km/s level (in high and medium resolution mode, respectively), paving the way to study of velocity fields in spectrally and spatially resolved object. It also provides a calibrated normalized spectrum, free of telluric lines, without the use of additional observations, since we use synthetic telluric spectra. The second improvement, regarding the correction of the atmospheric optical path difference jitter by post-processing of the fringe tracker recordings, will allow potentially a great improvement in precision and accuracy of the visibilities. This is not applicable to archival data, since these data are not yet recorded on a regular basis,but will be in a near future.

REFERENCES

[1] Petrov, R. G., Malbet, F., Weigelt, G., and *et al.*, "AMBER, the near-infrared spectro-interferometric three-telescope VLTI instrument," *A&A* **464**, 1–12 (Mar. 2007).

[2] Le Bouquin, J., Abuter, R., Bauvir, B., Bonnet, H., Haguenauer, P., di Lieto, N., Menardi, S., Morel, S., Rantakyrö, F., Schoeller, M., Wallander, A., and Wehner, S., "Fringe tracking at VLTI: status report," in [*Society of Photo-Optical Instrumentation Engineers (SPIE) Conference Series*], *Presented at the Society of Photo-Optical Instrumentation Engineers (SPIE) Conference* **7013** (July 2008).

[3] Wittkowski, M., Boboltz, D. A., Driebe, T., Le Bouquin, J., Millour, F., Ohnaka, K., and Scholz, M., "J, H, K spectro-interferometry of the Mira variable S Orionis," *A&A* **479**, L21–L24 (Feb. 2008).

[4] Absil, O., di Folco, E., Mérand, A., Augereau, J., Coudé du Foresto, V., Aufdenberg, J. P., Kervella, P., Ridgway, S. T., Berger, D. H., ten Brummelaar, T. A., Sturmann, J., Sturmann, L., Turner, N. H., and McAlister, H. A., "Circumstellar material in the Vega inner system revealed by CHARA/FLUOR," *A&A* **452**, 237–244 (June 2006).

[5] Kervella, P., Mérand, A., Perrin, G., and Coudé du Foresto, V., "Extended envelopes around Galactic Cepheids. I. l Carinae from near and mid-infrared interferometry with the VLTI," *A&A* **448**, 623–631 (Mar. 2006).

[6] Colavita, M. M., "Fringe Visibility Estimators for the Palomar Testbed Interferometer," *PASP* **111**, 111–117 (Jan. 1999).